Selenite-induced nitro-oxidative stress processes in *Arabidopsis thaliana* and *Brassica juncea*

Árpád Molnár+[1,2], Zsuzsanna Kolbert*+[1], Krisztina Kéri[1], Gábor Feigl[1], Attila Ördög[1], Réka Szőllősi[1], László Erdei[1]

[1] Department of Plant Biology, University of Szeged, Hungary

[2] Doctoral School in Biology, Faculty of Science and Informatics, University of Szeged, Szeged, Hungary

+ these authors contributed equally to this work

* corresponding author, Dr. Zsuzsanna Kolbert, kolzsu@bio.u-szeged.hu

Abstract

Extremes of selenium (Se) exert toxic effects on plants' physiological processes; although plant species tolerate Se differently. This study focuses on the effect of Se (0, 20, 50 or 100 μM sodium selenite) on secondary nitro-oxidative stress processes mainly using *in situ* microscopic methods in non-accumulator *Arabidopsis thaliana* and secondary Se accumulator *Brassica juncea*. Relative Se tolerance or sensitivity of the species was evaluated based on growth parameters (fresh and dry weight, root growth) and cell viability. Besides, selenite-triggered cell wall modifications (pectin, callose) and stomatal regulations were determined for the first time. In case of *Arabidopsis*, relative selenite sensitivity was accompanied by decreased stomatal density and induced stomatal opening, callose accumulation, pronounced oxidative stress and moderate nitrosative modifications. In contrast, the selenite-treated, relatively tolerant *Brassica juncea* showed larger number of more opened stomata, pectin accumulation, moderate oxidative and intense nitrosative stress. These suggest that selenite tolerance or sensitivity is rather associated with oxidative processes than secondary nitrosative modifications in higher plants.

Key words: *Arabidopsis thaliana; Brassica juncea*; cell wall modifications; nitro-oxidative stress; selenite.

1. Introduction

Selenium (Se) is a naturally occurring non-metal element, which is in many ways special and exists in many interchangeable oxidized and organic, inorganic forms. Elevated Se concentrations are naturally found in soils derived from Cretaceous shale rock (Kabata-Pendias, 1998) and Se may accumulate in the environment as the result of anthropogenic activities (Terry, 2000). Se shows chemical similarities with sulphur (S), therefore plants use their S uptake and metabolism system to assimilate Se. Some species in *Brassicaceae* family like *Brassica juncea* are sulphur loving and consequently are capable of accumulating larger amount of Se in their tissues (Pilon-Smits and Quinn, 2010). Additionally, these so-called secondary accumulators show reduced sensitivity to the presence of Se. On the other hand, most plant species, like the model plant *Arabidopsis thaliana* are non-Se-accumulators since they accumulate less than 25 μg Se/g dry weight and they cannot tolerate elevated Se levels in their environment (El-Ramady et al., 2015). Besides the plant species, also the applied Se form and the plants' age determine the rate of Se toxicity. The main consequences of Se excess, which are responsible for its toxicity, are the malformation of non-specific selenoproteins, reactive oxygen species (ROS) production and oxidative stress (Van Hoewyk, 2013). For the pro-oxidant properties of Se forms, the depletion of the major antioxidant, glutathione is principally responsible (Van Hoewyk, 2013). Also the disturbance in reactive nitrogen species (RNS) homeostasis and the consequent nitrosative stress are induced as the effect of Se (Lehotai et al., 2016a; Kolbert et al., 2016). The term RNS is used to describe the family of nitric oxide ($NO^{\cdot}$) originated molecules like, *inter alia*, peroxynitrite ($ONOO^{-}$), *S*-nitrosoglutathione (GSNO) or nitrogen dioxide radical ($^{\cdot}NO_2$) (Corpas et al., 2007). The intense production of RNS leads to macromolecule modifications resulting in nitrosative stress (Corpas et al., 2007; Valderrama et al., 2007). Posttranslational modification of proteins caused by tyrosine nitration is becoming a useful marker of nitrosative processes in plant systems (Corpas et al., 2013). Nitration of certain

tyrosine amino acids occurs in two steps resulting in the formation of 3-nitrotyrosine which induces alterations in protein structure and function and through the prevention of tyrosine phosphorylation it may influence signal transduction as well (reviewed by Kolbert et al., 2017).

Plants evolved protection mechanisms against damaging effects of excess Se such as the production and emission of volatile compounds like dimethyl(di)selenide (DMDSe) (El-Ramady et al., 2015). The rate of Se volatilization varies in plant kingdom which is determined also by the forms of Se (de Souza et al., 2000). In addition to protecting against Se toxicity within the plant tissues, Se volatilization may also have important ecological role like deterring herbivores and affecting neighbouring plants (Schiavon and Pilon-Smits, 2017a).

Several plant species are capable of modifying the chemical composition of their cell walls in order to prevent heavy metals from entering the cytoplasm. Increased formation and deposition of lignin or callose effectively reduces metal absorption thus facilitates plant survival and at the same time can partly be responsible for growth inhibition in metal-exposed environment (Le Gall et al., 2015). Moreover, heavy metal-triggered alterations in contents and methylesterification, acetylation status of pectins greatly determine heavy metal binding and the porosity of the cell wall thus its capability for growth (Le Gall et al., 2015).

Our research was motivated partly by the fact that Se-induced cell wall modifications and their possible correlations with Se tolerance are almost completely unknown. Similarly, our knowledge is incomplete regarding the regulatory effect of Se on stomata; although Se volatilization has been extensively studied in several plant species. Se has shown to induce nitro-oxidative stress in non-accumulator pea (Lehotai et al., 2016a), but the relationship between nitrosative processes and Se tolerance has not been examined so far. Our further aim was to evaluate the possible nitro-oxidative stress-inducing effect of selenite in non-accumulator *Arabidopsis thaliana* and secondary accumulator *Brassica juncea*.

2. Materials and methods

2.1.Plant growth conditions

Experiments were carried out with *Brassica juncea* L. Czern (cv. Negro Caballo) and *Arabidopsis thaliana* L. Heynh (Columbia-0). Seeds of both species were surface sterilised in 5% (v/v) sodium hypochlorite, then placed on perlite (in case of *Brassica* seeds) or on ½ Murashige-Skoog medium (in case of *Arabidopsis*) in Eppendorf tubes floating on Hoagland solution. In case of *Brassica*, the seedlings were pre-cultivated for nine days and then treated with 0 (control), 20, 50 or 100 μM sodium selenite (Na_2SeO_3) for one week meaning that *Brassica* plants were 16-days-old at the time of the sampling. In order to obtain the appropriate amount of biomass, *Arabidopsis* plants were grown in Hoagland solution for three weeks before being treated with the same selenite concentrations like mustard for one week. *Arabidopsis thaliana* plants were 28-days-old at the time of harvesting. Anoxia was prevented with constant aeration of the nutrient solution. Both plant species were grown during controlled conditions (150 μmol m^{-2}/s photon flux density, 12h/12h light/dark cycle, relative humidity 55–60% and temperature 25±2 ºC). All chemicals used during the experiments were purchased from Sigma-Aldrich unless stated otherwise.

2.2.Se content analysis

Leaf and root materials of *Arabidopsis* and *Brassica* were harvested separately and washed in distilled water then dried at 70 ºC for 72 hours. Nitric acid (65% w/v, Reanal, Hungary) and hydrogen peroxide (H_2O_2, 30%, w/v, VWR Chemicals, Hungary) were added to dried plant material. The samples were destructed at 200 ºC and 1600 W for 15 min. After appropriate dilutions, Se concentrations were determined by inductively coupled plasma mass spectrometry (ICP-MS) (Agilent 7700 Series, Santa Clara, USA). Se concentrations are given in μg/g dry weight (DW).

2.3.Evaluation of growth parameters, root system morphology and root cell viability

Fresh and dry weights of plant materials were measured using a balance and the values are given in mg. Primary root length was measured manually and expressed as centimetre. Also the number of visible lateral roots were counted manually and expressed as pieces/root.

In order to evaluate Se tolerance of the species, cell viability in root apical meristem was determined by using fluorescein diacetate (FDA) fluorophore according to Lehotai et al. (2011). Root tips were incubated in 10 μM FDA solution (prepared in 10/50 mM MES/KCl buffer, pH 6.15) for 30 min in darkness and were washed four times in buffer.

2.4.Microscopic visualization of cell wall modifications in the root system

Callose was detected with aniline blue fluorescent dye according to Cao et al. (2011) with slight modifications. The stain was used in 0.1% (w/v) solution containing 1 M of glycine. Root tips were incubated in dye solution for 5 minutes at room temperature, then washed once with distilled water.

Cell wall pectin content was visualized using 0.05% (w/v) ruthenium red (RR) solution prepared with distilled water. Root samples were incubated in RR solution for 15 minutes and were washed once with distilled water according to Durand et al. (2009).

2.5.Examination of stomatal parameters

Plant leaves were submerged in MES/KCl buffer (10/50 mM, pH 6.15) and the epidermal layers were carefully removed using forceps. In every case, strips were prepared from the same part of the leaf blade, avoiding leaf veins. The epidermal cell layers were put on slides using the previous buffer. Pictures were taken with a microscope (Zeiss Axiovert 200M) using 10x and 40x object lenses. Image analysis was carried out using Axiovision Rel. 4.8 software.

Stomatal density (pieces/mm^2) was analysed by counting all stomata in a 200 μm diameter circle. For the stomatal opening analysis, the widths of the stomatal pores were measured and the data are given as μm.

2.6.In situ detection of ROS, glutathione, cell-wall peroxidase activities, lipid peroxidation and RNS in the root tips

Dihydroethidium (DHE) at 10 μM concentration was applied for the detection of superoxide anion levels. Root segments were incubated in darkness at 37 ºC for 30 min, and washed two times with Tris-HCl buffer (10 mM, pH 7.4) (Kolbert et al., 2012).

Hydrogen peroxide levels were examined using 50 μM Amplex Red (10-acetyl-3,7 dihydroxyphenoxazine) dye solution in sodium phosphate buffer (50 mM, pH 7.5), then washed once with the same buffer according to Lehotai et al. (2012).

Cellular glutathione levels were detected with the help of monobromobimane (MBB) fluorophore. Root tips were stained in 100 μM dye solution (prepared in distilled water) for 60 min, and then washed once (Lehotai et al., 2016a).

Cell wall peroxidase (POD) activity was examined using 0.2% (w/v) pyrogallol solution containing 0.03% (v/v) hydrogen peroxide prepared in 10 mM phosphate buffer (pH 7.0). Samples were incubated for 15 minutes in room temperature and washed two times with distilled water (Eleftheriou et al., 2015).

Reactive aldehydes produced during lipid peroxidation were visualized using Schiff's reagent according to Arasimowicz-Jelonek et al. (2009). Root tips were incubated in dye solution for 20 minutes and then the reagent was replaced by 0.5% (w/v) $K_2S_2O_5$ (prepared in 0.05M HCl) for a further 20 minutes.

Nitric oxide level of the root tips was monitored with the help of 4-amino-5-methylamino- 2′,7′-difluorofluorescein diacetate (DAF-FM DA) according to Kolbert et al. (2012). Root segments were incubated in 10 μM dye solution for 30 min (darkness, 25±2 ºC), and washed twice with Tris-HCl (10 mM, pH 7.4).

Peroxynitrite was visualised with 10 μM dihydrorhodamine 123 (DHR) prepared in Tris-HCl buffer. After 30 min of incubation, root tips were washed with buffer two times (Sarkar et al., 2014).

Microscopic analysis of epidermal strips and stained root tips was accomplished under Zeiss Axiovert 200 M inverted microscope (Carl Zeiss, Jena, Germany) equipped with a high-resolution digital camera (AxiocamHR, HQ CCD, Carl Zeiss, Jena, Germany). Filter set 10 (exc.: 450–490, em.: 515–565 nm) was used for FDA, DAF-FM and DHR, filter set 9 (exc.:450–490 nm, em.:515–∞ nm) for DHE and Amplex Red and filter set 49 (exc.: 365 nm, em.: 445/50 nm) was applied for MBB and aniline blue. Circles of 100 μm radii were applied for measuring of the pixel intensity on digital photographs using Axiovision Rel. 4.8 software (Carl Zeiss, Jena, Germany).

2.7.Detection of nitrated proteins using SDS-PAGE and western blotting

Fresh leaf and root tissues of *Arabidopsis* and *Brassica* were grounded with double volume of extraction buffer (50 mM Tris–HCl buffer pH 7.6–7.8) containing 0.1 mM EDTA, 0.1% Triton X-100 and 10% glycerol and centrifuged at 12,000 rpm for 20 min at 4°C. The protein extract was treated with 1% protease inhibitor cocktail and stored at -20 °C. Protein concentration was determined using the Bradford (1976) assay with bovine serum albumin as a standard.

25 μg of denaturated root and shoot protein were subjected to sodium dodecyl sulphate-polyacrylamide gel electrophoresis (SDS-PAGE) on 12 % acrylamide gels. The proteins were

transferred to PVDF membranes using the wet blotting procedure (25 mA, 16h) for immunoblotting. After transfer, membranes were used for cross-reactivity assays with rabbit polyclonal antibody against 3-nitrotyrosine diluted 1:2000. Immunodetection was performed by using affinity isolated goat anti-rabbit IgG-alkaline phosphatase secondary antibody in dilution of 1:10000, and bands were visualized by using NBT/BCIP reaction. Nitrated bovine serum albumin served as positive control.

2.8.Statistical analysis

All results are shown as mean±SE. Data were statistically evaluated by Duncan's multiple range test (One-way ANOVA, $P \leq 0.05$) using SigmaPlot 12 or by Student's T-test applying Microsoft Excel 2010. All experiments were carried out at least two times with at least 3-10 samples each.

3. Results and Discussion

3.1. Se accumulation and translocation in selenite-treated *Arabidopsis* and *Brassica*

In the root and shoot tissues of both 28-days-old *Arabidopsis* and young *Brassica juncea* plants, Se concentration increased as the effect of exogenous selenite treatments (Fig 1AB). Total Se concentrations showed 28-, 125- and 300-fold accumulation in shoot tissues of 20, 50 and 100 μM selenite-treated *Arabidopsis*, respectively (Fig 1A). In *Brassica* shoots (Fig 1B), the degree of accumulation proved to be smaller (19-, 26- and 68-fold in case of 20, 50 and 100 μM selenite treatment, respectively) compared to *Arabidopsis*. In roots, Se accumulations were 70-, 128 and 220-fold in case of *Arabidopsis*, and 57-, 133- and 264-fold in case of 20, 50 and 100 μM selenite treated *Brassica*. This means that the Se accumulation capacity of young *Brassica juncea* roots a bit surpasses that of the older *Arabidopsis*. At the same time, it is quite surprising that the accumulation capacity of young, secondary Se accumulator *Brassica* plant is comparable with that of the older, non-accumulator *Arabidopsis*. This means that *Brassica* plants at the early growth stage do not show such rate of accumulation capacity that is typical for secondary accumulators. The roots of both species showed much higher Se contents compared to shoots and also the degree of accumulation proved to be higher in the root system than in the aerial plant parts, which is the result of the poor translocation capacity of selenite as described earlier (de Souza et al., 1998; Zayed et al., 1998). Indeed, selenite is retained in the root system where it is rapidly converted to organic forms, particularly to selenomethionine (Zayed et al., 1998).

3.2.Selenite affects organ development and viability of *Arabidopsis* and *Brassica*

The lowest applied selenite concentration did not influence shoot and root growth, while higher selenite doses significantly inhibited growth in both organs of mature (28-days-old) *Arabidopsis thaliana*. The shoot fresh weight decreased to one fifth and the root fresh weight

showed 50% reduction as the effect of 100 μM selenite (Fig 2AC), while in case of young *Brassica juncea* plants, 20 and 50 μM selenite did not decrease shoot fresh and dry weights and 100 μM Se caused diminution only in fresh weight but not in dry weight (Fig 2B). Both the 50 and the 100 μM Se resulted in serious (~50%) losses of root weights in *Arabidopsis* (Fig 2C), while in *Brassica,* 50 μM selenite reduced only fresh weight and 100 μM selenite resulted in significant fresh and dry weight reductions (root fresh weight was halved compared to control, Fig 2D). Therefore, critical Se concentration, which induces 50% growth reduction was ~120 μg/g dry weight in *Arabidopsis* and was ~250 μg/g dry weight in case of *Brassica* indicating the pronounced Se sensitivity of *Arabidopsis* comparted to *Brassica*. Moreover, in case of 50 and 100 μM selenite, leaf area, leaf number and petiole length decreased (Fig 2E, data not shown), but visible symptoms of selenite toxicity such as chlorosis or necrosis could not be observed in leaves of the species (Fig 2E). Indeed, asymptomatic Se accumulation in a wide concentration range is typical for many plant species (Gupta and Gupta, 2017).

As to the root system, primary root (PR) elongation, lateral root (LR) number and root meristem cell viability was determined in younger *Brassica juncea* and older *Arabidopsis thaliana* plants (Fig 3).

In *Arabidopsis*, 20 μM selenite did not cause PR shortening, but slightly induced LR formation (Fig 3A) resulting in larger fresh weight (Fig 2C). In *Brassica* root system, the positive effect of low Se dose was manifested in induced elongation of the primary root (Fig 3B). Moreover, 50 and 100 μM selenite resulted in a slight, non-significant induction of LR formation (Fig 3B). More severe selenite exposure (both 50 and 100 μM) led to the inhibition of PR elongation and to the reduction of LR number (Fig 3A) which together resulted in root weight loss (Fig 2C) of *Arabidopsis*, but only 100 μM Se was able to inhibit PR elongation and Se had no influence at all on LR emergence of *Brassica* (Fig 3B). The observed alterations in root developmental processes faithfully reflect Se tolerance (Tamaoki et al., 2008; Freeman et

al., 2010; Zhang et al., 2007) of *Brassica* and relative sensitivity of *Arabidopsis*. Selenite-induced inhibition of primary root elongation is partly due to the decrease in root apical meristem (RAM) cell division as it was observed in *Arabidopsis* model plant (Lehotai et al., 2016b).

Cell viability of the root meristem as an indicator of stress tolerance was determined by microscopy. All applied concentrations decreased viability in *Arabidopsis* root tips, while in case of *Brassica juncea*, 50 and 100 μM selenite caused only moderate viability loss (Fig 3CD). Besides inhibited cell division, the observed viability loss in RAM cells may also contribute to the growth inhibition at the organ level. In addition, the viability of RAM cells shows a good correlation with the Se tolerance or sensitivity of the plant species. Based on the effects of selenite on growth parameters, on PR elongation and on meristem cell viability, 28-days-old *Arabidopsis* plants showed sensitivity relative to younger *Brassica* plants, which is in accordance with earlier literature data (reviewed by Schiavon and Pilon-Smits, 2017).

3.3. Processes to reduce the amount of absorbed Se: stomatal regulation

The number and the opening of stomata determine the rate of Se volatilization, which is an effective way to reduce tissue Se content. Therefore, the density and the opening of stomata were examined in selenite-exposed *Arabidopsis thaliana* and *Brassica juncea* (Fig 4).

All applied selenite concentrations decreased the amount of stomata in *Arabidopsis* leaf epidermis (Fig 4A). In case of higher selenite doses, 1.5-times less stomata could be observed than in control plants (Fig 4 AEF); however, the sizes of stomatal apertures proved to be significantly larger as the effect of all applied selenite concentrations (Fig 4 CEF). In contrast, the lowest exogenous selenite concentration significantly increased both the sizes of stomatal apertures (Fig 4D) and the number of stomata per unit area (Fig 4B) in young *Brassica juncea* resulting in larger number of more opened stomata compared to control. Similarly, 100 μM

selenite caused enhancement of stomatal number and opening (Fig 4 BD). Microscopic images representing the data are shown in Fig 4 GH. Microscopic analysis of stomatal parameters is much less examined compared to stomatal conductance, which is determined by stomatal density and the stomatal size. Se treatments caused increased stomatal conductance in tobacco or in alfalfa (Jiang et al., 2015; Hajiboland et al., 2015). In other plants, like cucumber or maize, treatments with Se forms resulted in decreased stomatal conductance (Haghighi et al., 2016; Jiang et al., 2017) suggesting that the effect of Se forms on stomatal parameters depends on the examined species. In our experiments, the more tolerant *Brassica juncea* showed 20 and 100 μM selenite-induced increment in stomatal density and size supposedly creating decreased stomatal conductance and possibly contributing to enhanced Se volatilization. In hydroponically grown, 40 μM selenite-treated *Brassica juncea*, the rate of Se volatilization was 60 μg/g fresh weight/day (Van Huysen et al., 2003) on the basis of which it can be considered as well-volatilizing species (Terry et al., 1992). Moreover, the rate of volatilization was shown to correlate with endogenous Se content of the leaf (Terry et al., 1992) suggesting that Se or its volatile forms serve as direct signals for stomatal opening rather than an indirect regulation through the disturbance of water status. Although, regarding the complex signal mechanism of Se-regulated stomatal movements, we have no solid literature evidence yet. Occasionally purple discolorations appeared on the leaves of 100 μM selenite-treated *Brassica juncea*, which could be the results of anthocyanin accumulation (Fig 4 I) as it was reported in maize (Hawrylak-Nowak, 2008) or in purple lettuce (Liu et al., 2017). In the latter species, expressions of genes involved in anthocyanin biosynthesis like UDP glycose flavonoid glycosyl transferase (UFGT) and flavanone 3-hydroxylase (F3H) were upregulated by selenite (Liu et al., 2017). Because of their competitive uptake system selenite exposure may trigger phosphorous deficiency (Li et al., 2008) which in turn may result in purple pigmentation of the leaves. The accumulated anthocyanins can act as antioxidants, UV protectors or metal chelators (Winkel-Shirley, 2002).

297 Anthocyanin formation was visible in epidermis of *Brassica* leaves (Fig 4 IJ) where they can
298 interact with the metals (Landi, 2015) or in our case with the accumulated Se. Namely high
299 concentrations of Se were observed in large epidermal storage cells (Freeman et al., 2006;
300 2010), where anthocyanin accumulation seems also to be localized (Fig 4 IJ).

301 **3.4. Processes to reduce the amount of absorbable selenite in the root system: cell wall**
302 **modifications**

303 Modifications in cell wall composition and structure may contribute to tolerance in the
304 element-exposed environment and is concomitantly able to inhibit root growth. Pectin, callose
305 and lignin were microscopically visualized in lateral root tips of both plant species (Fig 5).

306 In the roots of four-weeks-old *Arabidopsis*, 20 and 100 μM selenite did not influence
307 pectin staining pattern of control root tips, while 50 μM selenite slightly increased pink
308 coloration indicating pectin presence in the meristem and root cap region (Fig 5A, indicated by
309 white arrowhead). In contrast, in 20 μM selenite-treated young *Brassica* roots, pectin staining
310 became remarkably intense in the whole lateral root (Fig 5B). In case of 50 and 100 μM selenite,
311 the intensified presence of pectin staining could be observed only in the elongation zone of the
312 LRs (Fig 5B). For the increase in pectin content, Se-triggered down-regulation of
313 pectinesterases (At5g04960; At2g45220; At3g10710) may be partly responsible as was found
314 in a transcriptome analysis of *Arabidopsis thaliana* (Van Hoewyk et al., 2008). Pectin may act
315 as a metal (e.g. Pb, Cd, Al) binding element of the cell wall contributing to the protection of
316 cytoplasm against high metal dosages (Polec-Powlak et al., 2007; Douchiche et al., 2010,
317 Hossain et al. 2006). Interestingly, in case of 20 μM selenite-treated *Brassica*, intensified
318 formation of pectin in lateral roots was accompanied by enhanced elongation. In general,
319 selenite-induced pectin formation was more intense in *Brassica* compared to *Arabidopsis*,

which supports that increased pectin content of root cell walls is a protection mechanism of tolerant plant species (El-Moneim et al., 2014).

The presence of callose in cell walls was evaluated by aniline blue staining (Fig 5C). In *Arabidopsis*, concentration-dependent callose accumulation (~3.5-fold) was detected in the root system while in cell walls of young *Brassica* roots was evident only in case of 100 μM selenite exposure and proved to be slighter (~1.8-fold) than in *Arabidopsis* roots (Fig 5C). Callose deposition causes the appearance of extra carbohydrate layers leading to thickening of the walls and consequently preventing the metal from entering the cytoplasm (Kartusch, 2003). Callose is synthetized by callose synthase the genes of which (Os01g48200.1; Os06g02260.2) were identified as putative Se responsive genes in *Lolium perenne* (Byrne et al., 2010). At the same time callose deposition at the site of plasmodesmata may inhibit molecule transport which in turn may contribute to growth inhibition (Zavaliev et al., 2011; Fig 3A). According to the literature, callose accumulation is typical for sensitive species (Llugany et al., 1994; Pirselová et al., 2012) like *Arabidopsis thaliana* in our experimental system (Fig 5C). Additionally, lignin deposition may be a protection mechanism in element-exposed environment (Le Gall et al., 2015). During one-week selenite treatment, lignification could not be microscopically observed either in *Arabidopsis* or in *Brassica* root system, but longer treatment period resulted in slight lignin deposition in tolerant *Brassica* (data not shown).

3.5. Selenite influences ROS levels, peroxidases and induces lipid peroxidation in the root system of *Arabidopsis* and *Brassica*

In the roots of *Arabidopsis,* the lowest applied selenite concentration resulted in significantly higher superoxide anion levels compared to control just like the more severe selenite doses (Fig 6A). In young *Brassica* roots, 20 and 50 μM selenite did not significantly influence superoxide levels, but 100 μM selenite exposure resulted in 2.5-fold formation of

superoxide anion compared to control (Fig 6B). Moreover, the levels of H_2O_2 increased as the effect of 50 μM selenite and showed a notable, 3-fold accumulation in 100 μM selenite-treated *Arabidopsis* roots (Fig 6C), but it showed a modest (1.5-fold) elevation only in 100 μM selenite-treated *Brassica* roots (Fig 6D). These results support that Se-compounds may evolve pro-oxidant effects disturbing the redox status of plant cells (Van Hoewyk, 2013). Intense formations of different ROS like superoxide radical and hydrogen peroxide were reported in both organs of several plant species (Tamaoki et al., 2008; Freeman et al., 2010; Lehotai et al., 2012; 2016ab; Chen et al., 2014; Dimkovikj and Van Hoewyk, 2014). Glutathione levels (examined in MBB-stained root tips) significantly decreased as the effect of the most severe applied Se treatment in *Arabidopsis* (Fig 6E), but both 50 and 100 μM selenite effectively decreased GSH content in *Brassica* roots (Fig 6F). Beyond the present experimental system, Se-triggered depletion of endogenous glutathione pool was observed in plant species like *Arabidopsis thaliana, Stanleya pinnata, Brassica napus, Pisum sativum* (Tamaoki et al., 2008; Freeman et al., 2010; Dimkovikj and Van Hoewyk, 2014; Lehotai et al., 2016). The reason for the selenite-triggered decrease in GSH content may be the interaction between reduced GSH and selenite yielding selenodiglutathione and superoxide radical (Terry et al., 2000; Schiavon and Pilon-Smits, 2017). This is supported by the increased formation of superoxide as the effect of 100 μM selenite treatment especially in *Brassica juncea* (Fig 6B). Glutathione is a major plant antioxidant (Noctor et al., 2012), therefore the decrease in its endogenous content can be a significant cause of Se-induced oxidative stress (Van Hoewyk, 2013). Additionally, since glutathione is associated with auxin transport and is involved in the maintenance of root growth (Koprivova et al., 2010), its depletion within the root tip tissues may contribute to the inhibition of root elongation in both plant species (Fig 3AB).

Brown pyrogallol staining indicates activity of cell-wall peroxidases (PODs), which were induced by all Se concentrations in *Brassica* (Fig 6H) and by 50 and 100 μM selenite in *Arabidopsis* (Fig 6G). Cell-wall peroxidases are involved in polymerization of lignin monomers using H_2O_2 (Siegel, 1953); however, their selenite-induced activation did not result in microscopically detectable lignification neither in *Arabidopsis thaliana* nor in *Brassica juncea* roots (data not shown). Cell wall-associated PODs also influence oxidative coupling reactions involving phenolics that are esterified to cell wall polysaccharides and formation of isodityrosine bridges that are thought to crosslink structural proteins (Fry, 1986). Based on their actions, PODs are considered to be involved in wall rigidification (Cosgrove, 1997) and thus their activation may result in growth inhibition (Fig 3AB). Pink staining showing the intensity of lipid peroxidation proved to be pronounced in 50 and 100 μM selenite-treated *Arabidopsis* root tips (Fig 6I). In *Brassica*, 50 μM selenite treatment caused only slight pink coloration in the root tip, while the highest applied selenite dose triggered more intense lipid peroxidation (Fig 6J). Enhanced formation of reactive oxygen species causes peroxidation of polyunsaturated fatty acids, yielding aldehydes such as 4-hydroxynonenal (4-HNE) and malondialdehyde (MDA) (Hartley et al. 1999). These aldehydic products of lipid peroxidation are widely accepted markers of oxidative stress and can be microscopically detected by Schiff's staining method (Pompella et al., 1987).

Results show that selenite proved to be pro-oxidant in both species. However, if we compare the susceptibility of the species with the degree of lipid peroxidation in the examined species, we can conclude that the sensitive *Arabidopsis* showed more intense selenite-induced lipid peroxidation compared to *Brassica juncea*. In case of both *Arabidopsis* and *Brassica*, peroxidation of lipids seems to be associated with the simultaneous formation of selenite-triggered superoxide and hydrogen peroxide in the root tips (Fig 6).

3.6. Selenite alters reactive nitrogen species levels in *Arabidopsis* and *Brassica* root tips

The formation of ROS is closely related to the production and signalling of reactive nitrogen species, therefore the level of RNS forms and their nitration effect on proteome was examined (Fig 7).

Milder selenite doses caused significant diminution of nitric oxide levels, while 100 μM selenite did not influence NO production in *Arabidopsis* root tips (Fig 7A). In young *Brassica* roots, none of the Se concentrations influenced NO levels (Fig 7B). The effects of Se forms on $NO^{\cdot}$ levels are diverse since selenite-induced $NO^{\cdot}$ production was reported in pea and *Brassica rapa* roots (Lehotai et al., 2016a; Chen et al., 2014), while similarly to the data of the present study, $NO^{\cdot}$ levels significantly decreased as the effect of Se exposure in other species like agar-grown *Arabidopsis* seedlings (Lehotai et al., 2016b). In the latter experimental system, data suggested that $NO^{\cdot}$ diminution was independent from nitrate reductase activity and selenite-induced cytokinin accumulation negatively influences $NO^{\cdot}$ levels (Lehotai et al., 2016b) possibly through a direct chemical reaction (Liu et al., 2013). In contrast, peroxynitrite-dependent fluorescence showed notable increment as the effect of all selenite concentrations in *Arabidopsis* (Fig 7C) and as the effect of higher Se doses in *Brassica* (Fig 7D). This means that selenite was able to induce its significant peroxynitrite production in the root system of both species; however, the rate of its accumulation seems to be related to Se sensitivity.

Protein tyrosine nitration as the consequence of peroxynitrite accumulation was examined in whole protein extracts of the shoot and root using western blot analysis (Fig 7E). In both organs of untreated *Arabidopsis* and *Brassica*, several protein bands showed immunoreactivity against 3-nitrotyrosine (Fig 7E) which indicates that in case of both species, both organs contain physiological tyrosine nitroproteome meaning that a certain protein pool is in nitrated state even under stress-free conditions. Similarly, basal tyrosine nitration in case of

417 control sunflower, pea and pepper plants have earlier been reported (Chaki et al., 2009; Begara-
418 Morales et al., 2013; Chaki et al., 2015). Based on the mostly negative impact of nitration on
419 protein activity (reviewed by Kolbert et al., 2017), physiological tyrosine nitroproteome of
420 healthy plants can be considered as an inactive part of the endogenous protein pool. Moreover,
421 protein pool of the control root system seems to be more affected by tyrosine nitration compared
422 to the shoot (Lehotai et al., 2016a) especially in *Arabidopsis* plants. In *Arabidopsis* shoot, signal
423 intensification of the immunoreactivity towards 3-nitrotyrosine antibody could be observed
424 only in 50 μM selenite-treated shoot sample in case of two bands (indicated by grey arrows).
425 In contrast, in *Brassica* shoots both 20 and 50 μM selenite caused intensified protein tyrosine
426 nitration in seven bands. In the root proteome, selenite-induced intensification of protein
427 nitration was observed in similar number of protein bands were observed in both species
428 (indicated by arrows), but the rate of Se-triggered nitration compared to controls proved to be
429 more intense in case of *Brassica* (Fig 7E). These indicate the pronitrant effect of exogenous
430 selenite treatment in both species; although it caused the appearance of newly nitrated protein
431 band neither in *Arabidopsis thaliana* nor in *Brassica juncea*. Surprisingly, selenite exerted more
432 severe effects on protein tyrosine nitration in both organs of young, more selenite tolerant
433 *Brassica* plants compared to older, relatively sensitive *Arabidopsis.* Protein tyrosine nitration
434 was formerly considered to be a biomarker for secondary nitrosative stress (Corpas et al., 2007;
435 2013) and as such may be related to the degree of impairment during stress. The more intense
436 Se-triggered protein tyrosine nitration as well as the notably high nitric oxide and peroxynitrite
437 levels (Fig 7BD) compared to *Arabidopsis* can be attributed to the young age of *Brassica juncea*
438 which may make it susceptible to nitrosative stress.

439

440

4. Conclusions

In the present experimental system, the effect of selenite exposure was examined in 16-days-old *Brassica juncea* and in older (4-weeks-old) *Arabidopsis thaliana* plants. Comparisons between the species therefore can only be made taking into account the age difference. Both examined plant lines took up selenite from the external medium and translocated it into the shoot system. Based on the slighter growth inhibition (fresh/dry weight, critical Se concentration, root length, lateral root number) and moderate viability loss, young *Brassica juncea* plants proved to be more tolerant to selenite exposure than older *Arabidopsis thaliana*. In case of *Arabidopsis*, relative selenite sensitivity was accompanied by decreased stomatal density and induced stomatal opening, callose accumulation, pronounced oxidative stress and moderate nitrosative modifications. In contrast, selenite-treated, relative tolerant *Brassica juncea* showed larger number of more opened stomata, pectin accumulation, moderate oxidative and intense nitrosative stress. These suggest that selenite tolerance or sensitivity is rather related to oxidative processes than secondary nitrosative modifications in higher plants.

Funding: This work was supported by the János Bolyai Research Scholarship of the Hungarian Academy of Sciences (Grant no. BO/00751/16/8) by the National Research, Development and Innovation Fund (Grant no. NKFI-6, K120383) and by the EU-funded Hungarian grant EFOP-3.6.1-16-2016-00008. Zs. K. was supported by UNKP-17-4 New National Excellence Program of the Ministry of Human Capacities.

5. References

Arasimowicz-Jelonek, M., Floryszak-Wieczorek, J., Kubiś, J., 2009. Involvement of nitric oxide in water stress-induced responses of cucumber roots. Plant. Sci. 177, 682–690.

Begara-Morales, J.C., Chaki, M., Sánchez-Calvo, B., Mata-Pérez, C., Leterrier, M., Palma, J.M., Barroso, JB., Corpas, F.J., 2013. Protein tyrosine nitration in pea roots during development and senescence. J. Exp. Bot. 64, 1121-1134. doi: 10.1093/jxb/ert006

Bradford, M.M., 1976. A rapid and sensitive method for the quantification of microgram quantities of protein utilizing the principle of protein-dye-binding. Anal. Biochem. 72, 248–255. doi: 10.1016/0003-2697(76)90527-3

Byrne, S.L., Durandeau, K., Nagy, I. et al., 2010. Identification of ABC transporters from *Lolium perenne* L. that are regulated by toxic levels of Se. Planta 231, 901-911. doi:10.1007/s00425-009-1096-y

Cao, Y., Lou, Y., Han, Y. et al., 2011. Al toxicity leads to enhanced cell division and changed photosynthesis in *Oryza rufipogon* L. Mol. Biol. Rep. 38, 4839. doi:10.1007/s11033-010-0618-9

Chaki, M., de Morales, P.Á., Ruiz, C., Begara-Morales, J.C., Barroso, J.B., Corpas, F.J., Palma, J.M., 2015. Ripening of pepper (*Capsicum annuum*) fruit is characterized by an enhancement of protein tyrosine nitration. Ann. Bot. 116, 637-47. doi:10.1093/aob/mcv016

Chaki, M., Valderrama, R., Fernández-Ocana, A.M., et al., 2009. Protein targets of tyrosine nitration in sunflower (*Helianthus annuus* L.) hypocotyls. J. Exp. Bot. 60, 4221–4234. doi: 10.1093/jxb/erp263

Chen, Y., Mo, H.-Z., Zheng, M.-Y., Xian, M., Qi, Z.-Q., Li, Y.-Q., et al., 2014. Se Inhibits Root Elongation by Repressing the Generation of Endogenous Hydrogen Sulfide in *Brassica rapa*. PLoS ONE 9, e110904. doi:10.1371/journal.pone.0110904

487 Corpas, F.J., Carreras, A., Valderrama, R., Chaki, M., Palma, J.M., del Río, L.A., Barroso, J.B.,
488 2007. Reactive nitrogen species and nitrosative stress in plants. Plant Stress 1, 37-41.
489 Corpas, F.J., Palma, J.M., del Río, L.A., Barroso, J.B., 2013. Protein tyrosine nitration in higher
490 plants grown under natural and stress conditions. Front. Plant. Sci. 4, 29. doi:
491 10.3389/fpls.2013.00029
492 Cosgrove, D.J., 1997. Assembly and enlargement of the primary cell wall in plants. Annu. Rev.
493 Cell. Dev. Biol. 13, 171–201. doi: 10.1146/annurev.cellbio.13.1.171
494 de Souza, M.P, Pilon-Smits, E.A.H., Lytle, C.M., Hwang, S., Tai, J., Honma, T.S.U., Yeh, L.,
495 Terry, N., 1998. Rate-limiting steps in Se assimilation and volatilization by Indian
496 mustard. Plant. Phys. 117, 1487–1494. doi: 10.1104/pp.117.4.1487
497 de Souza, M.P., Pilon-Smits, E.A.H., Terry, N., 2000. The Physiology and Biochemistry of Se
498 Volatilization by Plants. In: Ensley, B.D., Raskin, I. (Eds.), Phytoremediation of toxic
499 metals: Using plants to clean up the environment. Wiley & Sons, New York, pp 171-
500 190.
501 Dimkovikj, A., Van Hoewyk, D., 2014. Selenite activates the alternative oxidase pathway and
502 alters primary metabolism in *Brassica napus* roots: evidence of a mitochondrial stress
503 response. BMC Plant Biol. 14, 259. doi:10.1186/s12870-014-0259-6
504 Douchiche, O., Driouich, A., Morvan, C., 2010. Spatial regulation of cell wall structure in
505 response to heavy metal stress: Cadmium-induced alteration of the methyl-esterification
506 pattern of homogalacturonans. Ann. Bot. 105, 481–491. doi: 10.1093/aob/mcp306
507 Durand, C., Vicré-Gibouin, M., Follet-Gueye, M.L., Duponchel, L., Moreau, M., Lerouge, P.,
508 Driouich, A., 2009. The organization pattern of root border-like cells of *Arabidopsis* is
509 dependent on cell wall homogalacturonan. Plant Physiol. 150, 1411-21.
510 doi:10.1104/pp.109.136382

511 Eleftheriou, E.P., Adamakis, I.-D. S., Panteris, E., Fatsiou. M., 2015. Chromium-induced
512 ultrastructural changes and oxidative stress in roots of *Arabidopsis thaliana*. Int. J. Mol.
513 Sci. 16, 15852–15871. doi: 10.3390/ijms160715852
514 El-Moneim, D.A., Contreras, R., Silva-Navas, J., Gallego, J.F., Figueiras, A.M., Benito, C.,
515 2014. Pectin methylesterase gene and aluminum tolerance in *Secale cereal*. Environ.
516 Exp. Bot. 107, 125-133.
517 El-Ramady, H., Abdalla, N., Alshaal, T., et al., 2015. Se and its role in higher plants. In:
518 Lichtfouse, E., et al., (Eds.), Pollutants in Buildings, Water and Living Organisms,
519 Environmental Chemistry for a Sustainable World 7, Springer, pp 238-285. doi:
520 10.1007/978-319-19276-5_6
521 Freeman, J.L., Zhang, J.H., Marcus, M.A., Fakra, S., McGrath, S.P., Pilon-Smits, E.A.H., 2006.
522 Spatial imaging, speciation, and quantification of Se in the hyperaccumulator plants
523 *Astragalus bisulcatus* and *Stanleya pinnata*. Plant. Phys. 142, 124-134 doi:
524 10.1104/pp.106.081158
525 Freeman, J.L., Tamaoki, M., Stushnoff, C., Quinn, C.F., Cappa, J.F., Devonshire, J., Fakra,
526 S.C., Marcus, M.A., McGrath, S.P., Van Hoewyk, D., Pilon-Smits, E.A.H., 2010.
527 Molecular mechanisms of Se tolerance and hyperaccumulation in *Stanleya pinnata*.
528 Plant. Phys. 153, 1630-1652 doi: 10.1104/pp.110.156570
529 Fry, S.C., 1986. Cross-linking of matrix polymers in the growing cells of angiosperms. Annu.
530 Rev. Plant. Physiol. 37, 165–186. doi: 10.1146/annurev.pp.37.060186.001121
531 Gupta, M., Gupta, S., 2017. An overview of se uptake, metabolism, and toxicity in plants. Front.
532 Plant. Sci. 7, 2074 doi: 10.3389/fpls.2016.02074
533 Haghighi, M., Sheibanirad, A., Pessarakli, M., 2016. Effects of Se as a beneficial element on
534 growth and photosynthetic attributes of greenhouse cucumber. J. Plant. Nutr. 39, 1493-
535 1498.

536 Hajiboland, R., Rahmat, S., Aliasgharzad, N., Hartikainen, H., 2015. Se-induced enhancement
537 in carbohydrate metabolism in nodulated alfalfa (*Medicago sativa* L.) as related to the
538 glutathione redox state. Soil Sci. Plant. Nutr. 61, 676-687. doi:
539 10.1080/00380768.2015.1032181
540 Hartley, D.P., Kolaja, K.L., Reichard, J., Petersen, D.R., 1999. 4-Hydroxynonenal and
541 malondialdehyde hepatic protein adducts in rats treated with carbon tetrachloride:
542 immunochemical detection and lobular localization. Toxicol. Appl. Pharmacol. 161, 23-
543 33. doi: 10.1006/taap.1999.8788

544 Hawrylak-Nowak, B., 2008. Changes in anthocyanin content as indicator of maize sensitivity
545 to Se. J. Plant. Nutr. 31, 1232-1242.
546 Hossain, A.K.M.Z., Koyama, H., Hara, T., 2006. Growth and cell wall properties of two wheat
547 cultivars differing in their sensitivity to aluminium stress. J. Plant. Physiol. 163, 39–47.
548 Jiang, C., Zu, C., Shen, J., Shao, F., Li, T., 2015. Effects of Se on the growth and photosynthetic
549 characteristics of flue-cured tobacco (*Nicotiana tabacum* L.). Acta. Soc. Bot. Pol. 84,
550 71–77 DOI: 10.5586/asbp.2015.006
551 Jiang, J., Tang, X., Xue, Y., Lin, G., Xiong, Y.L., 2017. Dietary linseed oil supplemented with
552 organic Se improved the fatty acid nutritional profile, muscular Se deposition, water
553 retention, and tenderness of fresh pork. Meat. Sci. 131, 99-106.
554 Kabata-Pendias, A., 1998. Geochemistry of Se. J. Environ. Pathol. Toxicol. Oncol. 17, 173-
555 177.
556 Kartusch, R., 2003. On the mechanism of callose synthesis induction by metal ions in onion
557 epidermal cells. Protoplasma. 220, 219-225.

558 Kolbert, Zs., Pető, A., Lehotai, N., Feigl, G., Ördög, A., Erdei, L., 2012. *In vivo* and *in vitro*
559 studies on fluorophore-specificity. Acta. Biol. Szeged. 56, 37–41.

560 Kolbert, Zs., Lehotai, N., Molnár, Á., Feigl, G., 2016. "The roots" of Se toxicity: a new concept.
561 Plant. Signal. Behav. 11, e1241935. doi: 10.1080/15592324.2016.1241935

562 Kolbert, Zs., Feigl, G., Bordé, Á., Molnár, Á., Erdei, L., 2017. Protein tyrosine nitration in
563 plants: Present knowledge, computational prediction and future perspectives. Plant.
564 Physiol. Biochem. 113, 56–63.

565 Landi, M., 2015. Can anthocyanins be part of the metal homeostasis network in plant? Am. J.
566 Agr. Biol. Sci. 10, 170-177.

567 Le Gall, H., Philippe, F., Domon, J.-M., Gillet, F., Pelloux, J., Rayon, C., 2015. Cell wall
568 metabolism in response to abiotic stress. Plants. 4, 112-166.

569 Lehotai, N., Pető, A., Erdei, L., Kolbert, Zs., 2011. The effect of Se (Se) on development and
570 nitric oxide levels in *Arabidopsis thaliana* seedlings. Acta. Biol. Szeged. 55, 105–107.

571 Lehotai, N., Kolbert, Zs., Pető, A., Feigl, G., Ördög, A., Kumar, D., Tari, I., Erdei, L., 2012.
572 Selenite-induced hormonal and signaling mechanisms during root growth of
573 *Arabidopsis thaliana* L. J. Exp. Bot. 63, 5677–5687. doi: 10.1093/jxb/ers222

574 Lehotai, N., Lyubenova, L., Schröder, P., Feigl, G., Ördög, A., Szilágyi, K., Erdei, L., Kolbert,
575 Zs., 2016a. Nitro-oxidative stress contributes to selenite toxicity in pea (*Pisum sativum*
576 L.). Plant. Soil. 400, 107-122. doi: 10.1007/s11104-015-2716-x

577 Lehotai, N., Feigl, G., Koós, Á., Molnár, Á., Ördög, A., Pető, A., Erdei, L., Kolbert, Zs., 2016b.
578 Nitric oxide-cytokinin interplay influences selenite sensitivity in *Arabidopsis*. Plant.
579 Cell. Rep. 35, 2181-2195. Doi:10.1007/s00299-016-2028-5

580 Li, H.F., McGrath, S.P., Zhao, F.J., 2008. Se uptake, translocation and speciation in wheat
581 supplied with selenate or selenite. New. Phytol. 178, 92–102. doi:10.1111/j.1469-
582 8137.2007.02343.x

583 Liu, D., Li, H., Wang, Y., Ying, Z., Bian, Z., Zhu, W., Liu, W., Yang, L., Jiang, D., 2017. How
584 exogenous Se affects anthocyanin accumulation and biosynthesis-related gene
585 expression in purple lettuce?. Pol. J. Environ. Stud. 26, 717-722.
586 Liu, W.-Z., Kong, D.-D., Gu, X.-X., et al., 2013. Cytokinins can act as suppressors of nitric
587 oxide in *Arabidopsis*. PNAS. 110, 1548-1553. doi:10.1073/pnas.1213235110

588 Llugany, M., Massot, N., Wissemeier, A.H., Poschenrieder, C., Horst, W.J., Barceló, J., 1994.
589 Aluminium Tolerance of Maize Cultivars as Assessed by Callose Production and Root
590 Elongation. J. Plant. Nutr. Soil. Sci. 157, 447–451.

591 Noctor, G., Mhamdi, A., Chaouch, S., Han, Y., Neukermans, J., Marquez-Garcia, B., Queval,
592 G., Foyer, C.H., 2012. Glutathione in plants: an integrated overview. Plant. Cell.
593 Environ. 35, 454-84.
594 Pilon-Smits, E.A.H., Quinn, F.C., 2010. Se metabolism in plants. In: Hell, R., Mendel, R.-R.,
595 (Eds.), Cell Biology of Metals and Nutrients. Plant Cell Monographs 17, Springer-
596 Verlag Berlin Heidelberg, pp 225-241.
597 Piršelová, B., Veronika, Mistríková., Libantová, J., Moravčíková, J., Matušíková, I., 2012.
598 Study on metal-triggered callose deposition in roots of maize and soybean. Biologia 67,
599 698—705.
600 Polec-Powlak, K., Ruzik, R., Lipiec, E., Ciurzynska, M., Gawronska, H., 2007. Investigation
601 of Pb(II) binding to pectin in *Arabidopsis thaliana*. J. Anal. Atom. Spectrom. 22, 968–
602 972.
603 Pompella, A., Maellaro, E., Casini, A.F., Comporti, M., 1987. Histochemical detection of lipid
604 peroxidation in the liver of bromobenzene-poisoned mice. Am. J. Pathol. 129, 295–301.

605 Ribeiro, D.M., Silva Júnior, D.D., Cardoso, F.B., Martins, A.O., Silva, W.A., Nascimento,
606 V.L., Araújo, W.L., 2016. Growth inhibition by Se is associated with changes in primary

607 metabolism and nutrient levels in *Arabidopsis thaliana*. Plant. Cell. Environ. 39, 2235–
608 2246.
609 Sarkar, T.S., Biswas, P., Ghosh, K.S., Ghosh, S., 2014. Nitric oxide production by necrotrophic
610 pathogen *Macrophomina phaseolina* and the host plant in charcoal rot disease of jute:
611 complexity of the interplay between necrotroph-host plant interactions. PLOS One, 9,
612 e107348. doi:10.1371/journal.pone.0107348
613 Schiavon, M., Pilon-Smits, E.A.H., 2017. The fascinating facets of plant Se accumulation –
614 biochemistry, physiology, evolution and ecology. New. Phytol. 213, 1582–1596.
615 Siegel, S.M., 1953. On the biosynthesis of lignins. Physiol. Plant. 6, 134–139.

616 Tamaoki, M., Freeman, J.L., Pilon-Smits, E.A.H., 2008. Cooperative ethylene and jasmonic
617 acid signaling regulates selenate resistance in *Arabidopsis*. Plant. Phys. 146, 1219–1230.
618 Terry, N., Carlson, C., Raab, T.K., Zayed, A.M., 1992. Rates of Se volatilization amongst crop
619 species. J. Environ. Quality. 21, 341-344.
620 Terry, N., Zayed, A.M., de Souza, M.P., Tarun, A.S., 2000. Se in higher plants. Annu. Rev.
621 Plant. Physiol. Plant. Mol. Biol. 51, 401–432.

622 Valderrama, R., Corpas, F.J., Carreras, A., Fernández-Ocaña, A., Chaki, M., Luque, F., Gómez-
623 Rodríguez, MV., Colmenero-Varea, P., del Río, L.A., Barroso, J.B., 2007. Nitrosative
624 stress in plants. FEBS Lett. 581, 453-461.
625 Van Hoewyk, D., 2013. A tale of two toxicities: malformed selenoproteins and oxidative stress
626 both contribute to Se stress in plants. Ann. Bot. 112, 965–972.
627 Van Huysen, T., Abdel-Ghany, S., Hale, K.L., *et al.*, 2003. Overexpression of cystathionine-γ-
628 synthase enhances Se volatilization in *Brassica juncea*. Planta 218, 71-78

629 Winkel-Shirley, B., 2002. Biosynthesis of flavonoids and effects of stress. Curr. Opin. Plant.
630 Biol. 5, 218-23.

631 Zavaliev, R., Ueki, S., Epel, B.L., *et al.*, 2011. Biology of callose (β-1,3-glucan) turnover at
632 plasmodesmata. Protoplasma 248, 117-130.

633 Zayed, A., Lytle, C.M., Terry, N., 1998. Accumulation and volatilization of different chemical
634 species of Se by plants. Planta 206, 284–292.

635 Zhang, L., Ackley, A.R., Pilon-Smits, E.A.H., 2007. Variation in Se tolerance and accumulation
636 among 19 *Arabidopsis thaliana* accessions. J. Plant. Physiol. 64, 327-36.

637

638

Figures and captures

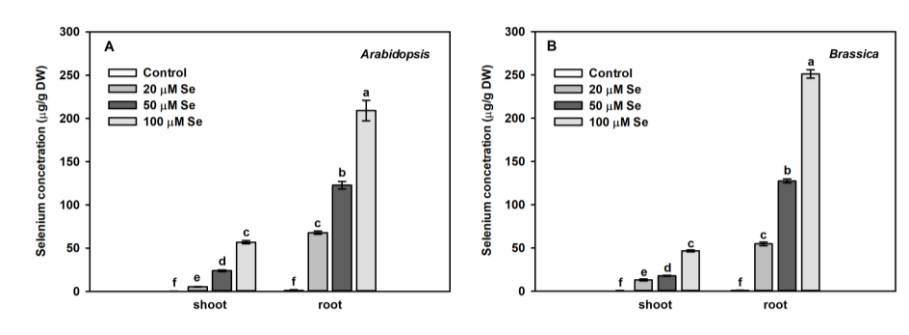

Fig 1 Concentrations of total Se in 28-days-old *Arabidopsis thaliana* (A) and 16-days-old *Brassica juncea* (B) treated with 0 (control), 20, 50 or 100 µM sodium selenite for 7 days. Different letters indicate significant differences according to Duncan's test (n=6, P≤0.05).

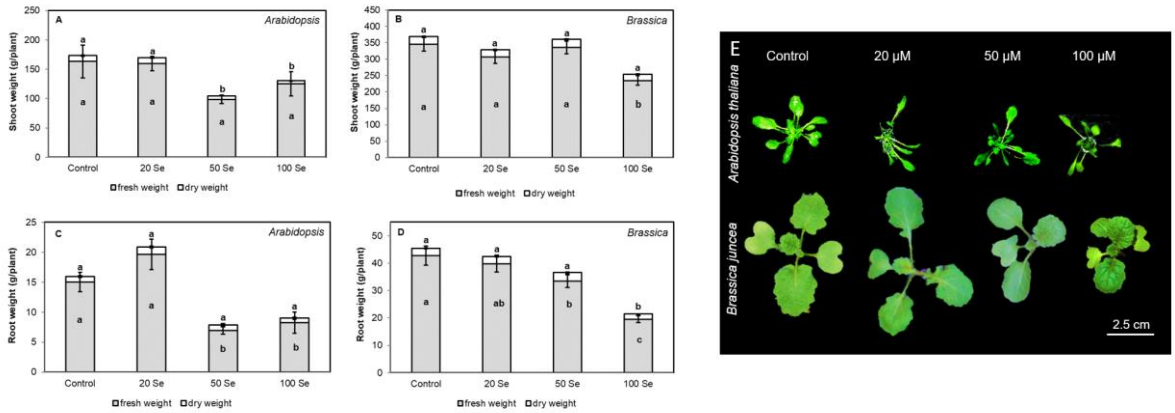

Fig 2 Shoot (A, B) and root (C, D) fresh and dry weights of control and selenite-treated 28-days-old *Arabidopsis* (A, C) and 16 days-old *Brassica* (B, D). Different letters indicate significant differences according to Duncan's test (n=20, P≤0.05). Representative images of control, 20, 50 or 100 µM selenite-treated *Arabidopsis thaliana* and *Brassica juncea* shoots (E). Bar=2.5 cm.

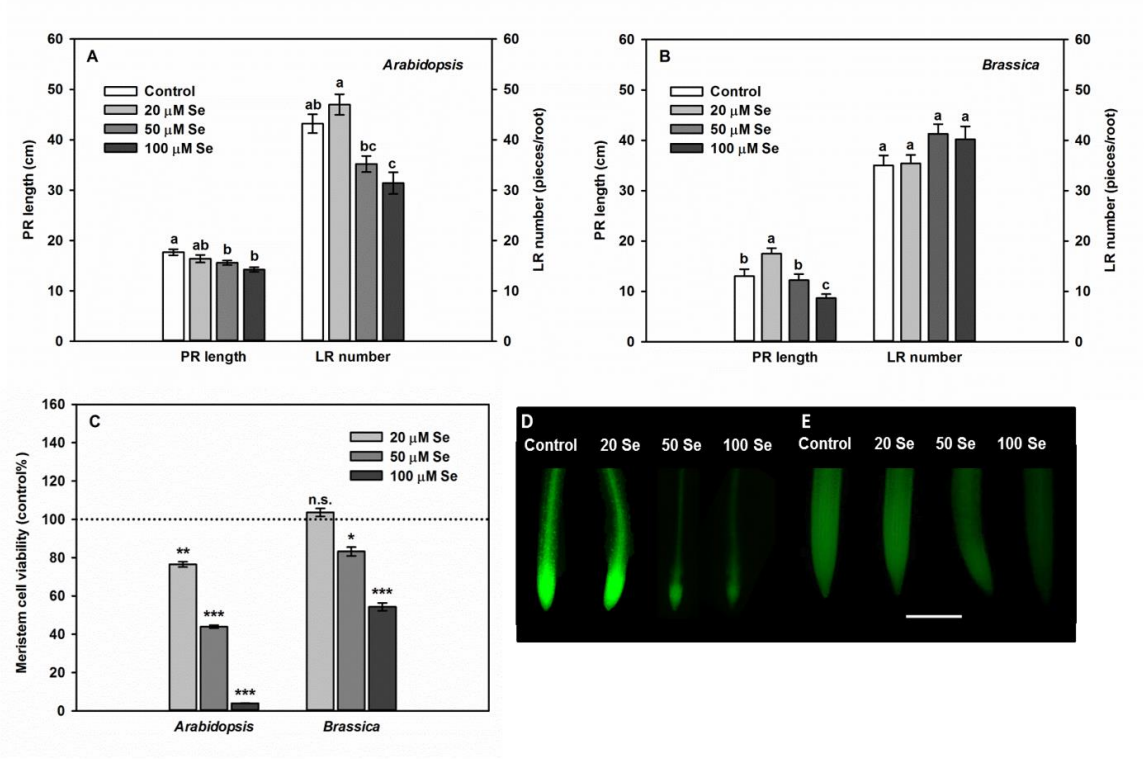

650

651 **Fig 3** Primary root length and lateral root number of 4-weeks-old *Arabidopsis thaliana* (A) and
652 16-days-old *Brassica juncea* (B) grown in hydroponics and treated with 0 (control), 20, 50 or
653 100 μM selenite for 7 days. Different letters indicate significant differences according to
654 Duncan's test (n=20, P≤0.05). (C) Cell viability of meristem cells in selenite-treated
655 *Arabidopsis* and *Brassica* roots. The lack of significance (n.s.) or significant differences
656 according to Student's t-test (n = 10, *P≤0.05, **P≤0.01, ***P ≤ 0.001) are indicated.
657 Representative fluorescent microscopic images of *Arabidopsis* (D) and *Brassica* (E) root tips
658 stained with fluorescein diacetate. Bar=200 μm.

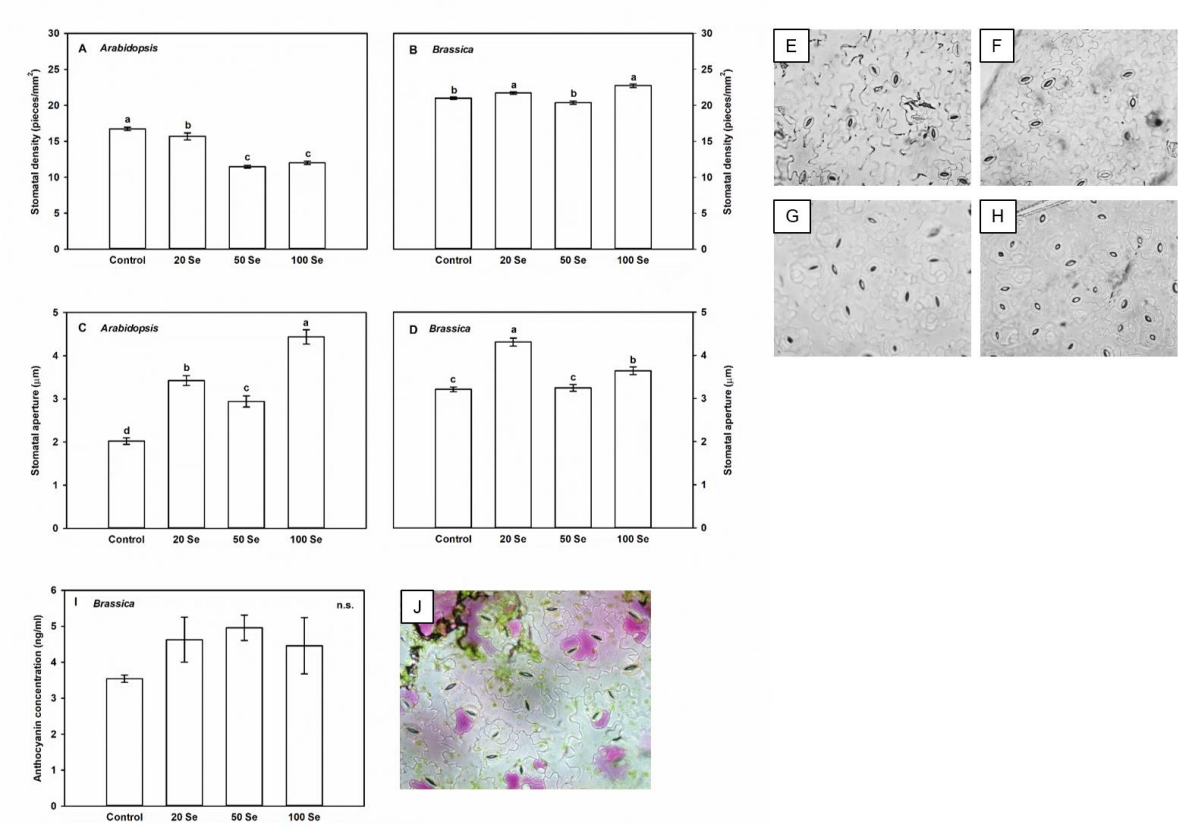

659

660 **Fig 4** Density (A, B) and size (C, D) of stomata in epidermis of *Arabidopsis* (A, C) and *Brassica*
661 (B, D) treated with 0 (control), 20, 50 or 100 μM selenite for 7 days. Different letters indicate
662 significant differences according to Duncan's test (n=200, P≤0.05). (E-H) Representative
663 images showing stomata of control (E, G) and 100 μM selenite-treated (F, H) *Arabidopsis*
664 *thaliana* (E, F) and *Brassica juncea* (G, H). Bars=50 μm. (I) Anthocyanin concentrations in the
665 leaves of control and selenite-treated 16-days-old, hydroponically grown *Brassica juncea*.
666 Statistical analysis was performed according to Duncan's test (n=6, P≤0.05) and n.s. indicates
667 non-significant differences. (J) Epidermal strip of 100 μM selenite-treated *Brassica juncea*.
668 Pink colorations indicate anthocyanin accumulation in large epidermal storage cells (red arrow).
669 Bar=50 μm.

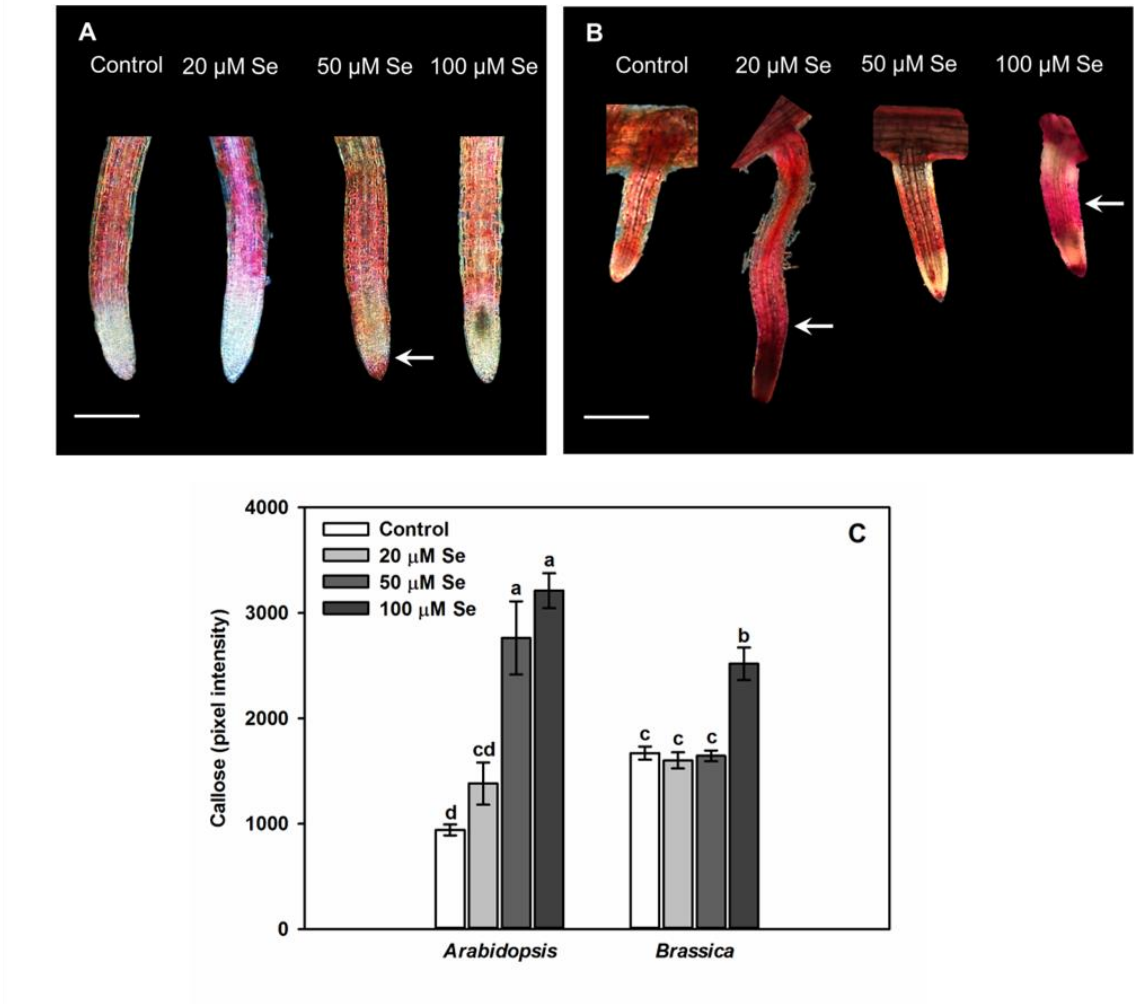

670

671 **Fig 5** Representative images showing pectin indicator ruthenium red staining in lateral root tips
672 of *Arabidopsis thaliana* (A) and *Brassica juncea* (B) treated with 0 (control), 20, 50 or 100 μM
673 selenite for 7 days in hydroponics (n=20, bars=150 μm). White arrows indicate intense signal
674 accumulation. (C) Fluorescent intensities of aniline blue indicating callose content in root tips
675 of control and selenite-treated *Arabidopsis* and *Brassica*. Different letters indicate significant
676 differences according to Duncan's test (n=10, $P \leq 0.05$).

677

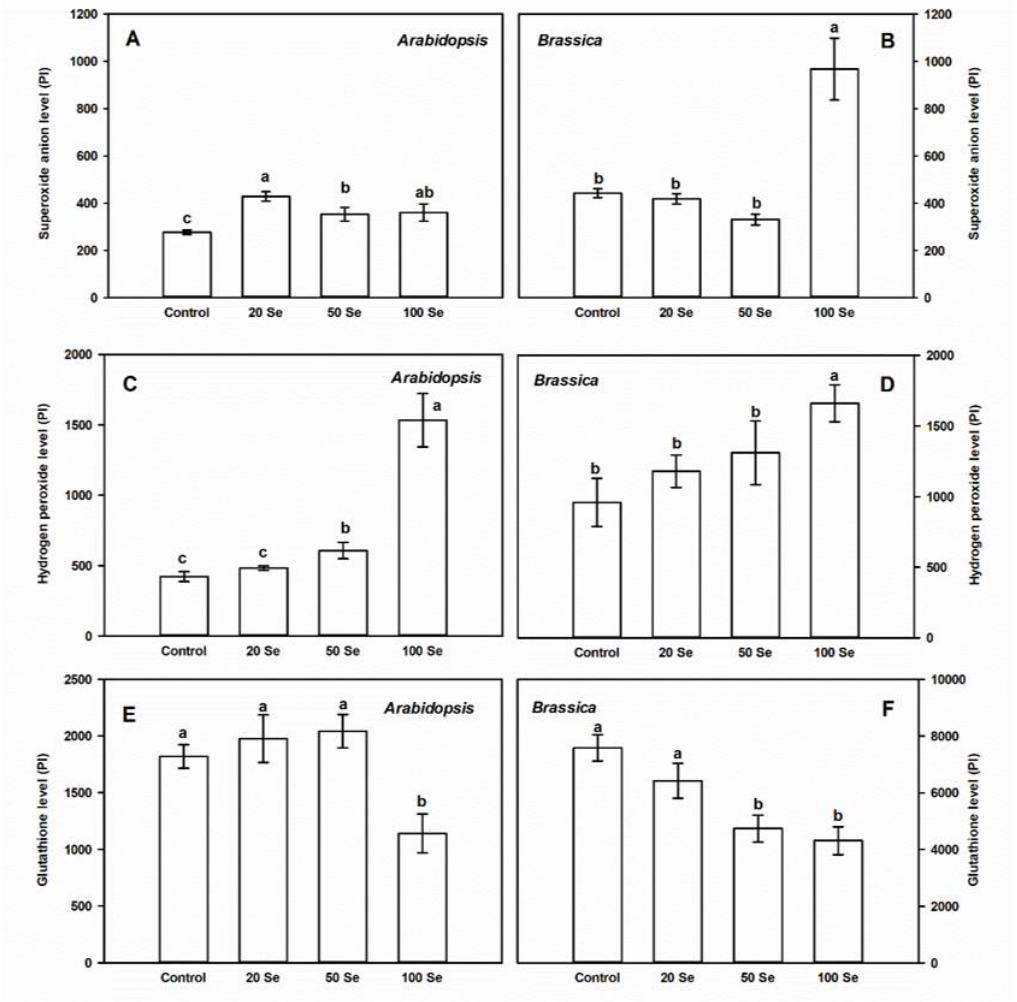
A
Arabidopsis
B
Brassica
Superoxide anion level (PI)
C
D
Hydrogen peroxide level (PI)
E
F
Glutathione level (PI)
Control
20 Se
50 Se
100 Se

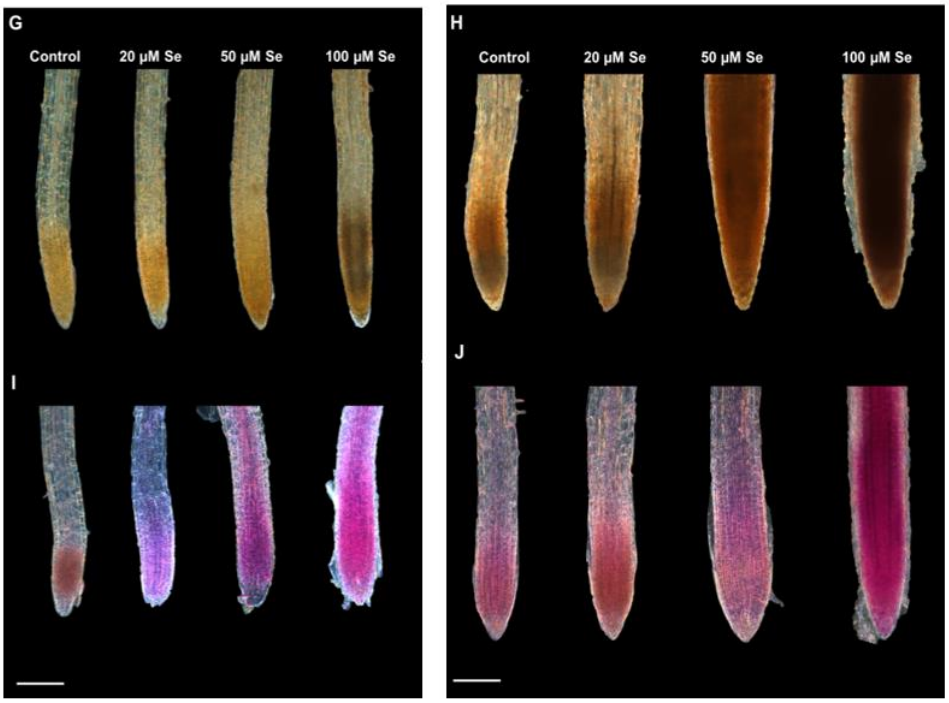
G
H
I
J
Control
20 µM Se
50 µM Se
100 µM Se

678

679 **Fig 6** Levels of superoxide (A, B), hydrogen peroxide (C, D) and glutathione (E, F) in root tips
680 of hydroponically-grown *Arabidopsis* (A, C, E) and *Brassica* (B, D, F) treated with 0 (control),
681 20, 50 or 100 µM selenite for 7 days. Different letters indicate significant differences according
682 to Duncan's test (n=10, P≤0.05). Microscopic images representing pyrogallol-stained root tips
683 of *Arabidopsis thaliana* (G) and *Brassica juncea* (H) indicating activities of cell-wall
684 peroxidases. Microscopic images of Schiff-reagent-labelled root tips of *Arabidopsis* (I) and
685 *Brassica* (J) indicating lipid peroxidation. Bars=150 µm.

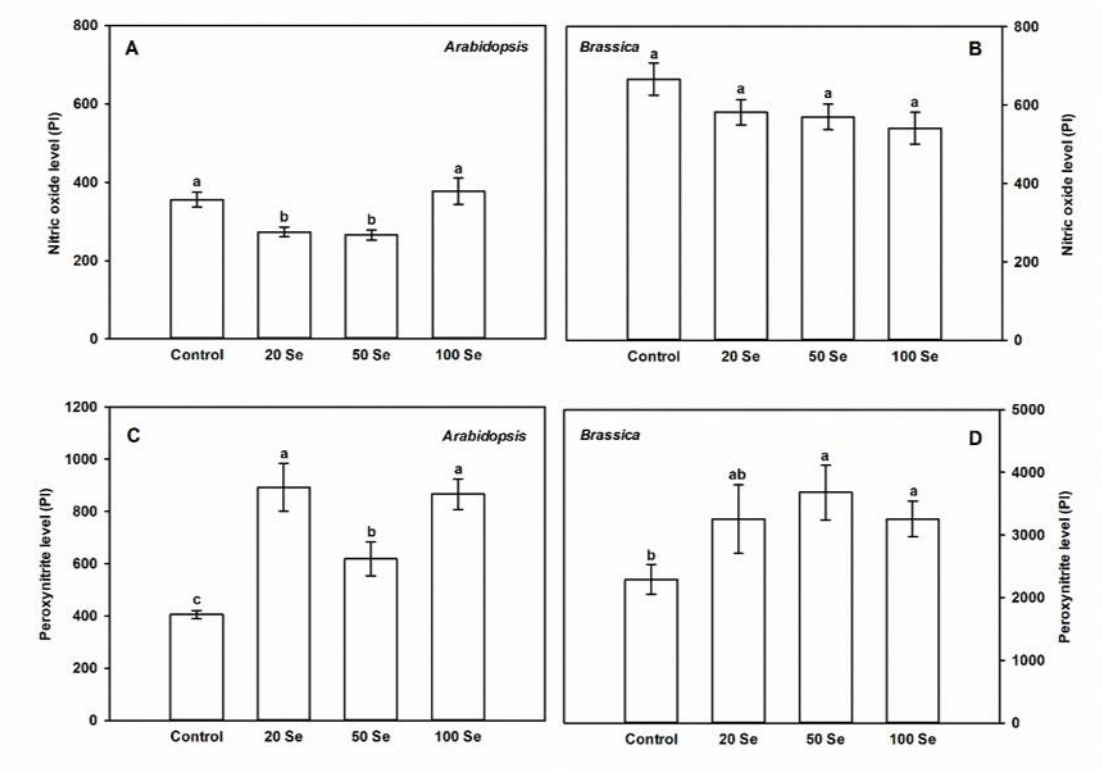
A
Arabidopsis
Nitric oxide level (PI)
800
600
400
200
0
a
b
b
a
Control
20 Se
50 Se
100 Se
B
Brassica
a
a
a
a
C
Arabidopsis
Peroxynitrite level (PI)
1200
1000
800
600
400
200
0
c
a
b
a
D
Brassica
5000
4000
3000
2000
1000
b
ab
a
a

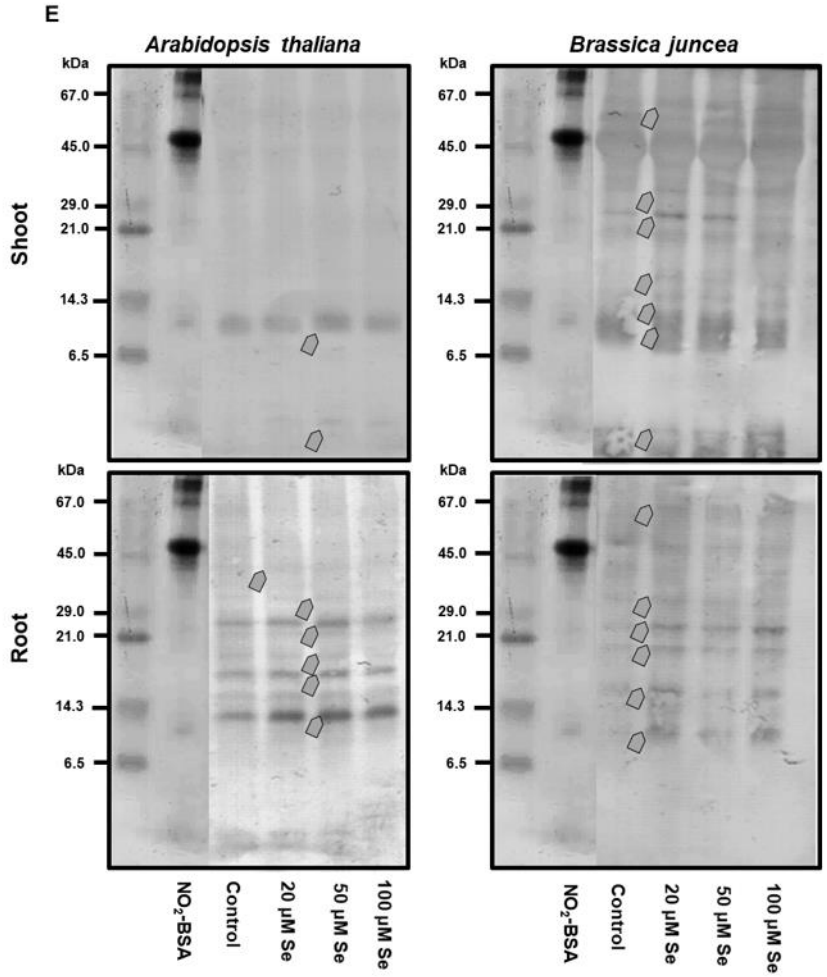
E
Arabidopsis thaliana
Brassica juncea
Shoot
Root
kDa
67.0
45.0
29.0
21.0
14.3
6.5
NO2-BSA
Control
20 µM Se
50 µM Se
100 µM Se

686

687 **Fig 7** Nitric oxide (A, B) and peroxynitrite (C, D) levels in the root tips of control and selenite-
688 treated *Arabidopsis* (A, C) and *Brassica* (B, D). Different letters indicate significant differences
689 according to Duncan's test (n=3, $P \leq 0.05$). (E) Representative immunoblots showing protein
690 tyrosine nitration in roots and shoots of *Arabidopsis* and *Brassica* under control conditions and
691 during 20, 50 or 100 μM selenite treatments. Root and shoot samples (25 μg protein) were
692 separated by SDS-PAGE and analysed by Western blotting with anti-nitrotyrosine antibody
693 (1:2000). Commercial nitrated BSA (NO_2-BSA) was used as a positive control. MM=molecule
694 marker. Arrows indicate protein bands showing selenite-induced intensification of
695 immunoreaction.
696
697
698
699